

# *Optimizing the thermal performance of building envelopes for energy saving in underground office buildings in various climates of China*

Article

Accepted Version

Creative Commons: Attribution-Noncommercial-No Derivative Works 4.0

Shi, L., Zhang, H., Li, Z., Luo, Z. and Liu, J. (2018) Optimizing the thermal performance of building envelopes for energy saving in underground office buildings in various climates of China. *Tunnelling and Underground Space Technology*, 77. pp. 26-35. ISSN 0886-7798 doi: <https://doi.org/10.1016/j.tust.2018.03.019> Available at <http://centaur.reading.ac.uk/76214/>

It is advisable to refer to the publisher's version if you intend to cite from the work. See [Guidance on citing](#).

To link to this article DOI: <http://dx.doi.org/10.1016/j.tust.2018.03.019>

Publisher: Elsevier

All outputs in CentAUR are protected by Intellectual Property Rights law, including copyright law. Copyright and IPR is retained by the creators or other copyright holders. Terms and conditions for use of this material are defined in the [End User Agreement](#).

[www.reading.ac.uk/centaur](http://www.reading.ac.uk/centaur)

**CentAUR**

Central Archive at the University of Reading

Reading's research outputs online

1     **Optimizing the thermal performance of building envelopes for energy saving in**  
2             **underground office buildings in various climates of China**

3     Luyang Shi<sup>1</sup>, Huibo Zhang<sup>2</sup>, Zongxin Li<sup>3</sup>, Zhiwen Luo<sup>4</sup>, Jing Liu<sup>1,5\*</sup>

4     <sup>1</sup>School of Municipal and Environmental Engineering, Harbin Institute of Technology, 202 Haihe  
5     Street, Nangang District, Harbin, China

6     <sup>2</sup>School of Naval Architecture, Ocean and Civil Engineering, Shanghai Jiao Tong University, 800  
7     Dongchuan Road, Minhang District, Shanghai, China

8     <sup>3</sup>The Fourth Design and Research Institute, Headquarters of the General Staff Corps, Beijing, China

9     <sup>4</sup>School of the Built Environment, University of Reading, Reading, United Kingdom

10    <sup>5</sup>State Key Laboratory of Urban Water Resource and Environment, Harbin Institute of Technology,  
11    Harbin, China

12

13

14

15

16

17    \*Corresponding author: Jing Liu

18    Address: School of Municipal and Environmental Engineering, Harbin Institute of Technology, No.73,  
19    Huanghe Road, Nangang District, Harbin 150000, China.

20    Tel./fax: +86 0451 8628 2123.

21    E-mail: liujinghit0@163.com

22

23 **Abstract** This article investigates the influence of the thermal performance of  
24 building envelopes on annual energy consumption in a ground-buried office building  
25 by means of the dynamic building energy simulation, aiming at offering reasonable  
26 guidelines for the energy efficient design of envelopes for underground office  
27 buildings in China. In this study, the accuracy of dealing with the thermal process for  
28 underground buildings by using the Designer's Energy Simulation Tool (DeST) is  
29 validated by measured data. The analyzed results show that the annual energy  
30 consumptions for this type of buildings vary significantly, and it is based on the value  
31 of the overall heat transfer coefficient (U-value) of the envelopes. Thus, it is necessary  
32 to optimize the U-value for underground buildings located in various climatic zones in  
33 China. With respect to the roof, an improvement in its thermal performance is  
34 significantly beneficial to the underground office building in terms of annual energy  
35 demand. With respect to the external walls, the optimized U-values completely  
36 change with the distribution of the climate zones. The recommended optimal values  
37 for various climate zones of China are also specified as design references for public  
38 office building in underground in terms of the building energy efficiency.

39 **Keywords:** Underground office buildings; Thermal performance; Optimization;  
40 China; DeST simulation

41

42

43

44

## 45 **1 Introduction**

46 In the view of the significant increases of the population in urban cities over recent  
47 decades, underground buildings have played an increasingly important role in the  
48 development and improvement of metropolises. A growing number of underground  
49 buildings, such as underground parking spaces, shopping malls, hospitals, railways,  
50 and office buildings, have been constructed as alternatives for urban area expansion in  
51 metropolises worldwide [1], and especially in China [2, 3]. For instance, the total area  
52 of underground space in Beijing has reached 72.68 million m<sup>2</sup> with a noted annual  
53 increase of over 7.3 million m<sup>2</sup> based on published figures in August 2014 [2]. The  
54 development of underground buildings effectively relieves land utilization in these  
55 mega cities, and definitely provides more living space for urbanites [4, 5]. Moreover,  
56 compared to buildings built above the ground, underground buildings may exhibit  
57 increased advantages in terms of building energy efficiency and indoor climate owing  
58 to their better capacities for heat storage, heat stability, and smaller temperature  
59 variations [6, 7]. Therefore, underground buildings require lower heating and cooling  
60 loads, save more energy for residents, and improve urban sustainability [6, 7, and 8].  
61 Many studies have demonstrated that underground buildings possess immense  
62 potential in reducing energy demands that can save more than 23% of energy in  
63 comparison with similar aboveground buildings [6, 9, 10, and 11]. It should be noted  
64 that the energy analysis of earth-sheltered domestic buildings situated in Poland  
65 showed that approximately 47%-80% reduction in the heating energy demand could  
66 be achieved by using various thickness of thermal insulation [6].

67 Recently, some researchers have attempted to study the energy performance of  
68 underground buildings using various research methods such as a two-dimensional  
69 transient finite element model (FEM) to investigate heat loss in a basement [12], a  
70 two-dimensional dynamic model of heat transfer through building envelopes using  
71 MATLAB [13], a combination of computer programs FlexPDE and EnergyPlus to  
72 simulate the heating and cooling energy demands in earth-sheltered buildings [6], a  
73 three-dimensional analysis of the thermal resistance of an external insulation system  
74 of a basement [13], a three-dimensional finite difference model (FDM) to verify the  
75 energy reduction potential of underground buildings [14], and an experimental  
76 analysis of indoor temperature variations related to ground layers in underground  
77 wine cellars [15]. All these experimental and simulated research studies indicate that  
78 the energy performance of underground buildings is determined by a wide variety of  
79 influential factors such as design typology, building function, HVAC systems,  
80 covering soil depth and type, thermal insulation, air infiltration [8]. In terms of design  
81 typology, contact surface area of building with the earth plays a key role in heat  
82 transfer. Overall, adopted methodologies have been more sophisticated as compared  
83 to conventional methodologies used for buildings above the ground. Additionally,  
84 these factors interact and change with different outdoor climates and indoor  
85 conditions [8, 16]. Among these factors, the building envelope is a factor that can be  
86 easily designed and optimized in the early design stages for energy efficiency.

87 In terms of building envelope features for aboveground buildings, an improvement  
88 in the thermal performance of the envelope, such as an increase in the thermal

89 insulation level, can effectively reduce heat loss, and the annual energy demands for  
90 both heating and cooling [17, 18]. The efficiency requirements for building envelopes,  
91 such as the assembly's maximum U-value (overall heat transfer coefficient), are  
92 determined for building energy efficiency based on the ASHRAE Standards 90.1–  
93 2016 [19] in America, and GB50189–2015 in China [20]. However, the heat transfer  
94 through an underground building is completely different from that of a building that is  
95 above the ground because the soil's thermal properties are treated as a thermal  
96 reservoir for modulating interior temperatures [21]. Therefore, these standards  
97 correspond to buildings built above the ground and might be not suitable for  
98 underground buildings in which the thermal performance of the envelopes is designed  
99 for energy efficiency.

100 In this context, several researchers have focused on the investigation of the  
101 influence of the thermal performance of the envelopes on energy consumption with  
102 respect to heating and cooling loads for underground buildings [11, 13, 22, and 23].  
103 Krarti and Choi demonstrated that additional insulation is required at the corners, as  
104 opposed to the middle section of the surface to minimize the heat loss for  
105 underground buildings, and that insulation material should be close to the soil surface  
106 [13]. Yuan et al. evaluated the effect of building materials on the temperature and heat  
107 flux for envelopes in a basement, and indicated that the thermal conductivity of  
108 building materials is an important factor in the heat transfer of the envelopes [22].  
109 Dronkelaar stated that the energy performance is more significantly dependent on the  
110 U-value of the constructions and the ventilation rates in certain colder climates [11].

111 Staniec and Nowak suggested that thinner thermal insulation, elicits a better cooling  
112 effect gained from the soil, whereas a thicker insulation leads to a smaller heating  
113 energy demand [6, 23]. These studies indicates that the thermal performance of the  
114 envelopes in an underground building is one of the most important design criteria to  
115 allow the best thermal comfort effect [8]. However, the relationships between the  
116 annual energy demand and the thermal performance of the envelopes in underground  
117 buildings might not be very accurate and explicit, especially with respect to various  
118 climatic zones. In general, outdoor climatic conditions have a slight influence on the  
119 indoor environment and energy demand for underground buildings in a short time.  
120 However, the long-term distribution of ground temperature is crucial in determining  
121 the energy demand, which is dependent on the climate and soil's thermal properties.  
122 Although the simulated analysis by Staniec and Nowak illustrated the influence of  
123 thermal insulation on heating and cooling loads, the combined effect of thermal  
124 performance of the envelope on the annual energy demand (including heating and  
125 cooling energy) has not been considered in their study. Furthermore, their simulation  
126 was only performed for Polish climate conditions, and thus, it may not be possible to  
127 apply their conclusions to various climates around the world.

128 On the other hand, China has a vast territory spanning five different climatic  
129 conditions [24]. Specifically, temperature waves of underground spaces differ in  
130 terms of values, amplitude, period, and phase displacement for various climatic zones.  
131 Therefore, the efficiency requirements of building envelopes in an underground  
132 building may vary significantly with changes in the climate. Hence, a reasonable and



133 formal guideline, or a standard listing the efficiency requirements, are necessary for  
134 underground building envelopes in various climates to provide a basis for the  
135 energy-saving design of the envelopes, which is currently lacking in China.

136 The aim of this study is to investigate the influence of the thermal performance of  
137 the envelopes on annual energy consumption for underground office buildings in  
138 various climatic zones of China, thereby allowing the determination of the optimized  
139 U-value for building envelopes (including the roof and the exterior wall), and  
140 introducing reasonable guidelines for the energy efficient design of underground  
141 building envelopes. First, a building energy simulation tool known as the Designer's  
142 Energy Simulation Tool (DeST) was presented in detail to deal with the thermal  
143 process for the underground building and the accuracy of DeST is also validated by  
144 measured data. Thus, DeST is used to calculating the hourly heating and cooling loads  
145 for ground-buried office buildings in this study to optimize the thermal performance  
146 of the insulation configurations of envelopes for various climatic zones in China,  
147 based on the annual energy consumption.

## 148 **2 Methodology**

149 This section is organized in four parts. Section 2.1 describes the details for  
150 simulating thermal process within underground buildings by means of DeST. Section  
151 2.2 presents a prototype underground building model implemented in the DeST  
152 platform. Section 2.3 shows the classification of climate zones in China and lists the  
153 ten major Chinese cities selected for this simulation. The evaluation method of

154 calculating annual energy demand based on hourly heating and cooling loads is  
155 summarized in Section 2.4.

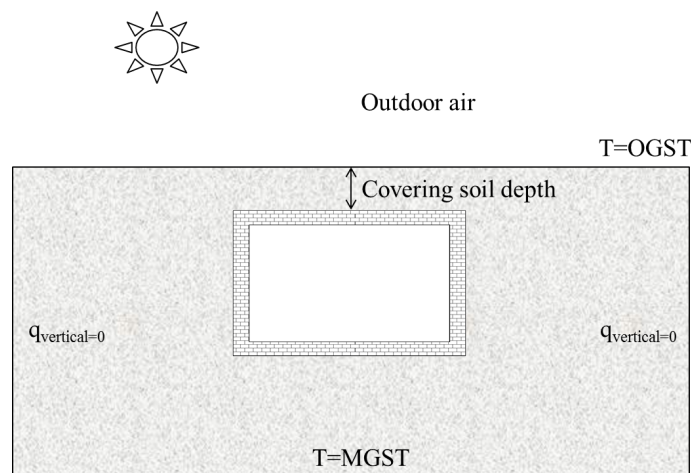
## 156 **2.1 Simulation tool**

157 DeST is an effective building energy simulation tool that was developed by  
158 Tsinghua University in 1989. To-this-date, numerous case analyses and theoretical  
159 validations are performed, and as a result, DeST has become a widely-used platform  
160 for calculating building thermal processes and for dynamic simulations of the  
161 building's energy distribution. Specifically, DeST develops a graphical user interface  
162 that is based on AutoCAD for all simulation processes to avoid additional modelling  
163 work and information loss due to conversion [25].

164 In terms of energy performance, the most significant difference between an  
165 underground building and an aboveground building is that all the building partitions  
166 are in contact with soil, rather than atmosphere. Therefore, it is critical to determine  
167 surrounding ground temperature and calculate the heat transfer process of  
168 ground-coupled envelopes that are in contact with the earth for simulating an  
169 underground building. Generally, heat transfer within ground-coupled envelope is  
170 computed using numerical methods, such as FEM and FDM [12, 14]. However, these  
171 models are excessively time-consuming for hourly simulations over the period of a  
172 year [25].

173 In DeST simulation, the heat transfer process of ground-coupled envelopes (the  
174 envelopes that are contact with the earth) is decomposed into three processes which

175 are controlled by ground-coupled envelope surface temperature, outdoor ground  
 176 surface temperature and temperature difference of ground-coupled envelope surfaces  
 177 [26]. The schematic diagram of heat transfer within ground-coupled envelopes is  
 178 presented in Fig.1. Outdoor ground surface temperature (OGST) is mainly determined  
 179 by above air temperature, absorbed solar radiation, long wave radiation with sky.  
 180 Ground-coupled envelope surface temperature is mainly determined by room air  
 181 temperature, long wave radiation with occupant, light, equipment and other inner  
 182 surface in the room. Temperature of deep soil surface is set as constant and  
 183 approximately equals to mean ground surface temperature (MGST).



184

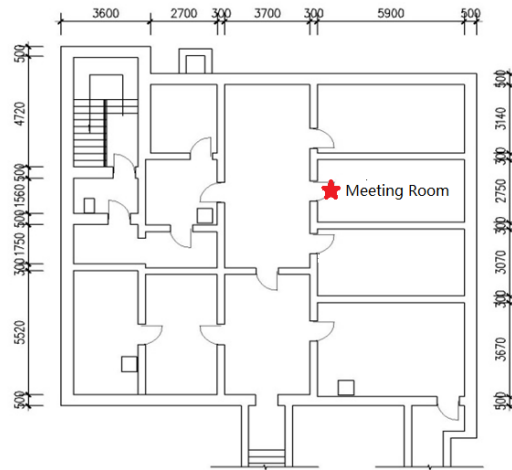
185 Fig.1 Schematic program of underground building's heat transfer and boundary condition (not in scale)

186 In the first process, outdoor ground surface temperature is set as zero and the  
 187 temperature of other ground-coupled envelopes is set the same as the selected one.  
 188 The heat transfer process controlled by ground-coupled envelope surface temperature  
 189 is computed by one-dimensional Equivalent Slab. In the second process, temperature  
 190 of all ground-coupled envelope surfaces is set as zero and outdoor ground surface  
 191 temperature is simplified as a constant and 1 year period harmonic variable. In the

192 third process, outdoor ground surface temperature is set as zero and the temperatures  
193 of ground-coupled envelopes are different. The heat between ground-coupled  
194 envelopes is exchanged through the soil and is computed by a one-dimensional Extra  
195 Partition Wall. Therefore, replace the ground-coupled envelope in a room using  
196 Equivalent Slab and treat the heat flux computed in the second and third process as  
197 heat source of Equivalent Slab inner surface, and thus the heat transfer of  
198 ground-coupled envelope is calculated and implemented into building thermal  
199 simulation. This approach can save a large amount of time for the full-year calculation  
200 compared with other numerical methods [26].

## 201 **2.2 Underground office building details**

202 All simulation stages are performed in DeST for a simplified prototype building  
203 model based on a typical large-scale office building that is fully underground. The  
204 building is located at a depth of 1.0 m below the ground in Beijing and has only one  
205 underground floor with a story height of 3.3 m. The building is consisted of five  
206 sections as detailed in a previous study [27]. Fig.2 shows the layout of the eastern  
207 section of the building as the chosen prototype building model in the calculation,  
208 which has a building area of 215.5 m<sup>2</sup>. Table 1 lists the components and thermal  
209 performance of the building envelope. The building is surrounded by rammed clay  
210 that is considered as a special component for the exterior walls. The thermal  
211 conductivity coefficient of rammed clay is 1.16 W/(m·K).



212

213

Fig.2 The layout of the simplified underground building (unit: mm)

214

Table 1 Components and the thermal performance of the building envelope

Building envelope	Building envelope components	U-value (W/m <sup>2</sup> ·K)
Roof	20 mm Lime mortar + 300 mm reinforced concrete	0.81
External walls	30 mm Lime mortar + 200 mm reinforced concrete	1.00

215

In this simulation, the layout and building structure are constructed using model parameters that are as close as possible to the real-life situation [28]. It is assumed that there is no infiltration or solar gains for the underground building because the building is completely buried beneath the surface.

219

Three scenarios are considered in the simulation. The details of building characteristics for the three scenarios are presented in Table 2. Scenario A is performed to simulate annual indoor temperature variations in the meeting room as depicted in Fig.2. Scenarios B and C are both executed to calculate the hourly load of the underground building. First, Scenario B is performed to investigate the influence of the U-value of the roof on the annual energy demand, and to determine its optimal U-value. This is followed by the execution of Scenario C to optimize the thermal

225

226 performance of the exterior walls. It should be noted that the U-value of the roof for  
 227 Scenario C is adopted based on the optimized results in Scenario B. In this study, two  
 228 covering soil depths (1.0 m and 3.0 m) (calculated between the rooftop of the  
 229 building and the ground surface) are chosen because the depth also greatly affects the  
 230 indoor heat environment of the subsurface structure [8]. In this simulation, the  
 231 research objective is the public office building, thus the parameters of the thermal  
 232 disturbances (Table 3) from the occupants, illumination, and equipment in the  
 233 building are assumed to be the same as those of public buildings above the ground  
 234 according to Chinese national standard for public buildings [20], which is typical and  
 235 representative for office buildings. The schedules for the interior heat sources are  
 236 described in Table 4. Mechanical ventilation does not consider the impact of fresh air  
 237 on the heat transfer between the building and surrounding envelopes. Therefore, the  
 238 fresh air load is not included in the simulation for the calculation of the annual hourly  
 239 load.

240 Table 2 Building characteristics for the three executed scenarios

Scenario	Depth (m)	U-value of the roof (W/m <sup>2</sup> ·K)	U-value of the exterior wall and floor(W/m <sup>2</sup> ·K)	Internal heat gains
A	3.0	0.81	1.00	None
B	1.0/3.0	Variable value	1.00	See Table 3
C	1.0/3.0	Optimal value	Variable value	See Table 3

241 Notes: Variable values: 0.22/0.49/0.81/1.00/1.50/2.00/2.45/2.97, optimal value: the optimized results of  
 242 U-value for the roof in Scenario B.

243 Table 3 Internal heat sources for an underground building

Building function	MNP(people/m <sup>2</sup> )	MI(W/m <sup>2</sup> )	MHGFE (W/m <sup>2</sup> )
-------------------	-----------------------------	-----------------------	---------------------------

Public office	0.1	9.0	15
---------------	-----	-----	----

244 Notes: MNP: maximum number of individuals, MI: maximum illumination, MHGFE: maximum heat  
 245 gain from the equipment.

246 Table 4 Schedules for various internal heat sources

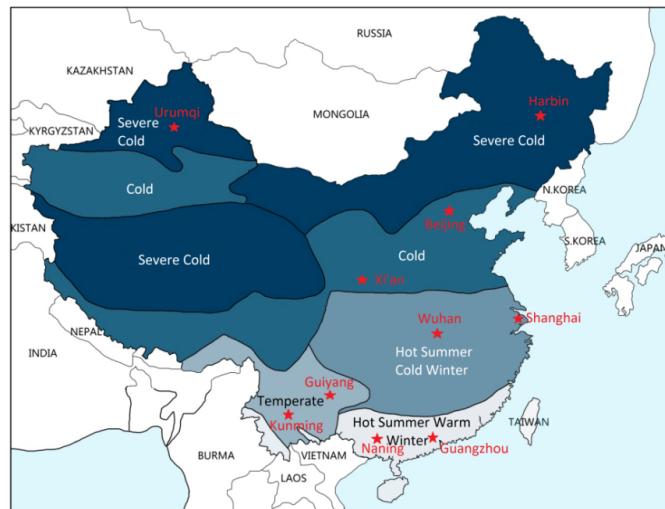
Interior disturbance	Schedule
Occupants	ON from 08:00 to 17:00 on workday, OFF at all other times
Illumination	ON from 08:00 to 17:00 on workday, OFF at all other times
Equipment	ON from 08:00 to 17:00 on workday, OFF at all other times

247 For Scenarios B and C, the heating and cooling systems have considered the  
 248 provision of a comfortable indoor environment in an underground building. The high  
 249 heat storage capacity of the surrounding soil results in an indoor underground  
 250 temperature that is lower than 20 °C sometimes even during the summer [15, 27], and  
 251 it is then necessary to heat the room. Thus, it is not suitable to simply set the same  
 252 parameters for an underground space to those used for indoor air conditioning for  
 253 buildings above the ground, such as 26 °C in the summer, and 20 °C in winter. In the  
 254 simulation, the indoor temperatures of an underground building in the summer and  
 255 winter were set to a wide range of temperatures that approximately spanned 20-28 °C,  
 256 and 18-22 °C, respectively.

### 257 **2.3 Climatic zones in China**

258 Based on the different climatic characteristics, China is divided into five major  
 259 climate zones as follows: a severe cold zone (SCZ), a cold zone (CZ), a hot summer  
 260 and cold winter zone (HSCWZ), a hot summer and warm winter zone (HSWWZ), and  
 261 a temperate zone (TZ) (Fig.3). This climatic classification framework is principally

262 based on the average temperatures in the coldest and hottest months [18].



263

264 Fig.3 Classification of climate zones in China and geographic locations of the 10 major cities selected  
265 for this study, as denoted by the red stars

266 For Scenario B and C, 10 typical cities covering the climate zones are selected for  
267 the investigation, and they are denoted using red stars, as shown in Fig.3. They  
268 represent the corresponding climatic zones. The meteorological data for these cities  
269 during a typical meteorological year is determined based on a multiyear weather  
270 database file [16]. In DeST, hourly data of weather variations is calculated in a similar  
271 manner to the calculation of the weather input parameters for Scenario B and C.

## 272 2.4 Annual energy demand calculation

273 The hourly heating and cooling loads for the underground building are obtained  
274 based on the calculations of Scenario B and C. The grades of energy used in the  
275 heating and cooling systems as well as their energy efficiencies are different. It is  
276 necessary to convert the various energy forms to electricity power by using the



277 method detailed in the GB50189–2015 Standard [20], and thus annual energy  
278 consumption for underground building is obtained.

279 For all the climatic zones, space cooling is provided using water-cooled  
280 centrifugal chillers [20], and the electricity consumption for cooling can be calculated  
281 in accordance to Eq.(1):

$$282 \quad E_C = \frac{Q_C}{A \times SCOP_T} \quad (1)$$

283 where,  $Q_C$  denotes the accumulative cooling load on the calculated DeST results in  
284 kWh,  $A$  denotes the total cooling areas in  $m^2$ , and  $SCOP_T$  is the synthetic coefficient  
285 of performance for the cooling system and equals to 2.5 [20].

286 The heating system is determined based on the climate zones. The system  
287 operation with a coal-fired boiler is applied in the SCZ and CZ, while the system that  
288 operated with a natural-gas-fired boiler is applied in all the other climate zones [23].  
289 The electricity consumption for the heating system can be evaluated using Eqs.(2) and  
290 (3), respectively.

$$291 \quad E_H = \frac{Q_H}{A \eta_1 q_1 q_2} \quad (2)$$

292 where,  $Q_H$  denotes the annual accumulative heating load based on the calculated  
293 results of DeST in kWh,  $A$  denotes the total heating areas in  $m^2$ ,  $\eta_1$  denotes the  
294 synthetic efficiency of the heating system with a coal-fired boiler and equals to 60%  
295 [20],  $q_1$  denotes the calorific value of standard coal and equals to 8.14 kWh/ kgce,  
296 and  $q_2$  denotes the coal consumption rate in the power generation and equals to  
297 0.360 kgce/kWh.

$$298 \quad E_H = \frac{Q_H}{A \eta_2 q_3 q_2} \varphi \quad (3)$$

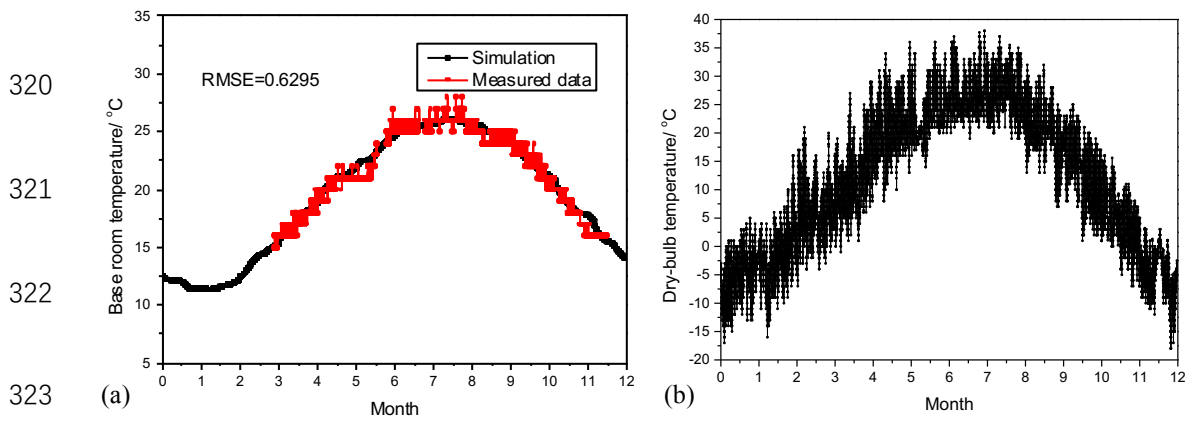
299 Where,  $\varphi$  denotes the converted coefficient between standard coal and gas, and  
300 equals to  $1.21 \text{ kgce} / \text{m}^3$ ,  $\eta_2$  denotes the synthetic efficiency of the heating system  
301 with a natural gas-fired boiler and equals to 75% [20], and  $q_3$  denotes the calorific  
302 value of gas and equals to  $9.87 \text{ kWh} / \text{kgce}$ .

303 Finally, the annual energy consumption is the sum of  $E_H$  and  $E_C$ , and is  
304 considered as the evaluation index of the total energy consumption for a full year in  
305 this study.

### 306 **3 Results and discussions**

#### 307 **3.1 Analysis of room temperature simulation**

308 Basal room temperature refers to the indoor temperature that arises from the  
309 thermal interaction between the outdoor climatic conditions and the building in its  
310 natural state [16]. In this case, there were no heating/cooling sources or working  
311 HVAC systems. In this study, the meeting room, denoted as a red star in Fig.2, was  
312 used as an example to analyse the indoor temperature variations throughout the entire  
313 year. Fig.4 (a) shows the measured indoor temperature data a period of 9–10 months,  
314 while the outdoor temperature variations of Beijing during the year at which tests  
315 were conducted are shown in Fig.4 (b). Additionally, the annual hourly basal room  
316 temperature of the meeting room was calculated using DeST (Scenario A), as  
317 presented in Fig.4 (a). It should be noted that the meteorological data for Scenario A  
318 were based on a weather database file that matched the year at which the tests were  
319 conducted.



324 Fig.4 Basal temperature variations in the meeting room for simulation and measurements (a) and  
 325 annual hourly dry-bulb temperature in Beijing during the testing year at which tests were conducted (b)

326 A sinusoidal behaviour of seasonal variability in the indoor temperature of the  
 327 meeting room is distinctly observed in Fig.4. A comparison of the variations of indoor  
 328 and outdoor temperatures indicates that their behaviours are almost identical in terms  
 329 of the exhibited tendencies to monthly changes, but the temperature waves differ in  
 330 terms of values, amplitude, and phase displacement [15]. First, the indoor temperature  
 331 is very stable throughout the year eliciting a mean temperature of approximately  
 332 20 °C when compared to the outdoor temperature owing to the thermal inertia of the  
 333 surrounding soil. The highest temperature of the underground space is approximately  
 334 10 °C lower than that of the outdoor air, while the lowest temperature of underground  
 335 space is more than 20 °C larger than that of outdoor air. Additionally, the highest  
 336 indoor temperature in underground buildings occurred in early August, while the  
 337 highest outdoor temperature occurred in early July. Similarly, the lowest indoor  
 338 temperature of the underground space is observed in mid-February, while the lowest  
 339 outdoor temperature is observed in mid-January. This implies that the phase  
 340 displacement between the indoor temperature in the underground space (at a depth of

341 1.0 m below the ground) and the outdoor temperature approximately corresponds to  
342 one month.

343 In order to compare the calculated and measured indoor temperature of the  
344 meeting room, we calculated the coefficient of variation of the root-mean square error  
345 (RMSE) using the following equation:

$$346 \quad \text{RMSE} = \sqrt{\sum_{i=1}^N (T_{meas} - T_{model})^2 / N}$$

347 (4)

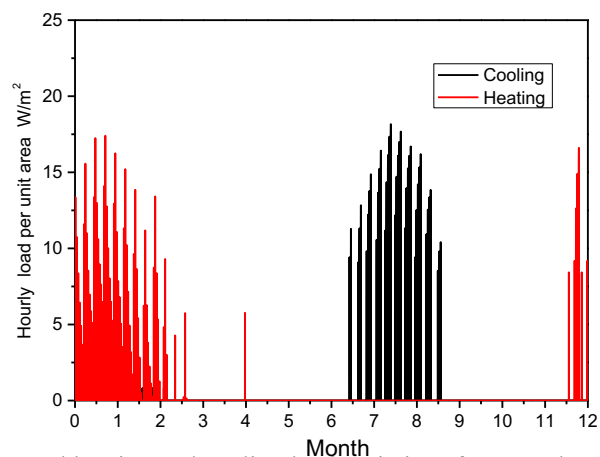
348 where,  $T_{meas}$  is the measured indoor temperature at a given time,  $T_{model}$  is the  
349 modelled indoor temperature at that same time, and  $N$  is the number of measurements.

350 The value of RMSE is used to quantify the agreements between measured and  
351 computational results and this value in Fig.4 (a) is 0.63, showing there is a good  
352 agreement between that experimental and computational results. Thus, the accuracy of  
353 the thermal process within underground buildings by means of DeST-based dynamic  
354 simulation is thus validated.

### 355 **3.2 Analysis of hourly load for heating and cooling.**

356 In this section, the calculated results for Scenario C are analyzed and illustrated as  
357 an example. In this case, the details of the simulation are as follows: the building is  
358 located at a depth of 1.0 m below the ground (Beijing), and the heat transfer  
359 coefficient of the roof is 0.8 W/(m<sup>2</sup>·K). Fig.5 shows the simulation results for the  
360 distribution of annual hourly heating and cooling loads in an underground building.

361 In Fig.5, it is observed that the cooling load started at the end of July and lasted  
 362 until the beginning of September, and this indicated that the cooling system worked  
 363 during this period to regulate the indoor temperature to preset levels. The onset of the  
 364 cooling operation occurred a month later than that used for buildings built above the  
 365 ground. This may be owing to the phase displacement of the ground temperature  
 366 compared to the outdoor temperature. A similar tendency in the heating load is also  
 367 observed in Fig.5. For an underground building, the heating system mainly worked  
 368 from January to February instead of the coldest months with respect to the outdoor  
 369 atmosphere in Beijing (December and January).



370  
371  
372  
373  
374  
375 Fig.5 Annual heating and cooling load variations for an underground building

### 376 3.3 Impact of thermal characteristics of the roof on building energy demand

377 In this section, the influence of the thermal performance of the roof on the  
 378 building's energy demand is analyzed for various climatic zones, based on the  
 379 calculated results of Scenario B. Fig.6 (a)-(e) indicates that the annual energy demand  
 380 changes as a function of the U-values of the roof for each of the corresponding  
 381 climatic zones. As shown, the relationships between annual energy consumption and

382 U-values for the roofs for various climatic zones of China are very similar. Overall,  
383 the decrease in the U-values of the roof effectively reduced the building's energy  
384 demand by enhancing the thickness of the thermal insulation. This can be explained  
385 by the fact that the existing insulation diminished the impacts of the outdoor climate  
386 on the indoor environment of an underground space. For example, in Harbin (with a  
387 building depth of 1.0 m), the amount of annual energy consumption decreased from  
388  $6.20 \text{ kW}\cdot\text{h}/\text{m}^2$  to  $3.55 \text{ kW}\cdot\text{h}/\text{m}^2$ , and this corresponded to a change of approximately  
389 42.7% when the U-value decreased from  $2.0 \text{ W}/(\text{m}^2\cdot\text{K})$  to  $0.5 \text{ W}/(\text{m}^2\cdot\text{K})$ . The  
390 effectiveness of the U-value is more significant at lower values, while U-values  
391 higher than  $2.5 \text{ W}/(\text{m}^2\cdot\text{K})$  minimized their impacts on the building's energy  
392 consumption.

393 Therefore, the analyzed results reveal that the energy efficiency requirements for  
394 the roofs of underground buildings are consistent with the standards for buildings  
395 above the ground. Thus, an improvement in the thermal performance of a roof, based  
396 on the increase of the insulation materials, is beneficial to the building's energy  
397 consumption. As shown in Fig.6 (a) and (b), it is also clear that additional insulation  
398 materials are required for cold climatic zones-and especially for SCZ to minimize heat  
399 loss through the roof, and especially for shallow-buried underground buildings.

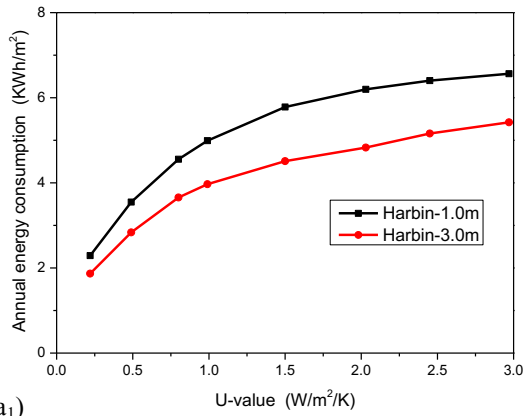
400

401

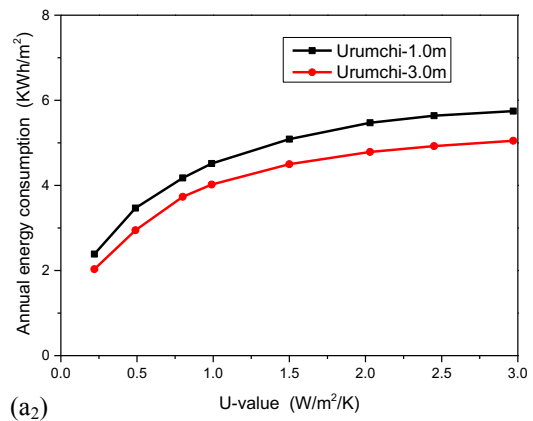
402

403

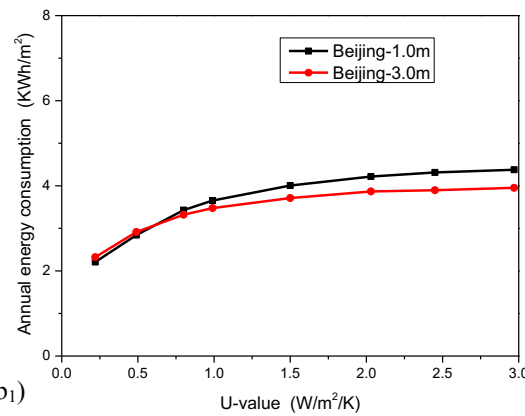
404



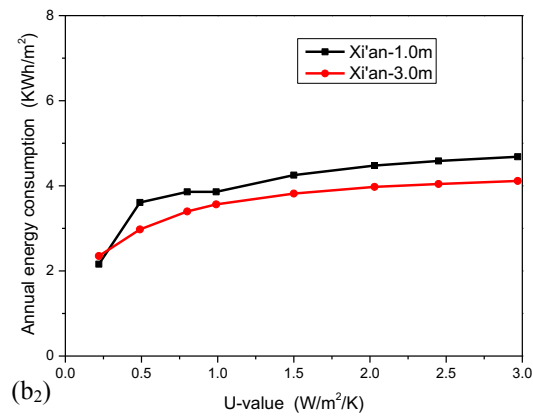
405



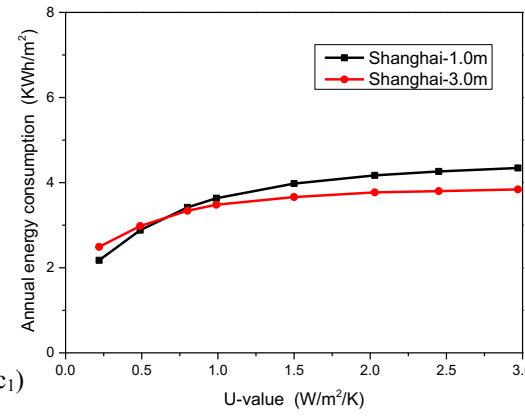
406



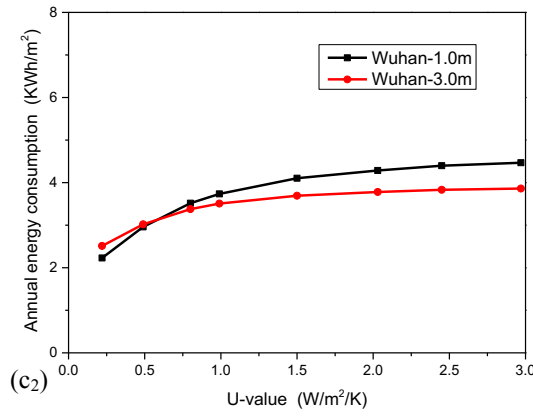
407



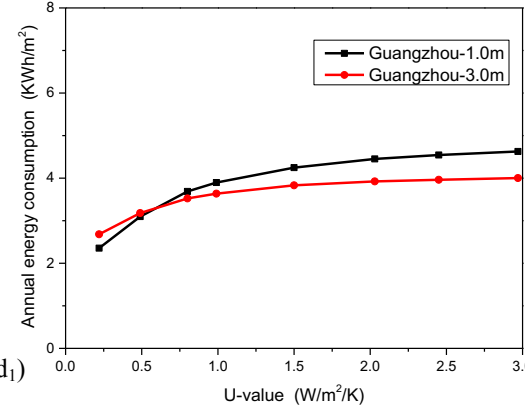
408



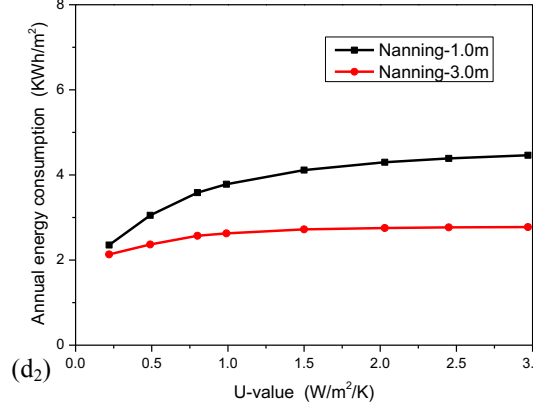
409



410



411



412

413

414

415

416

417

418

419

420

421

422

423

424

425

426

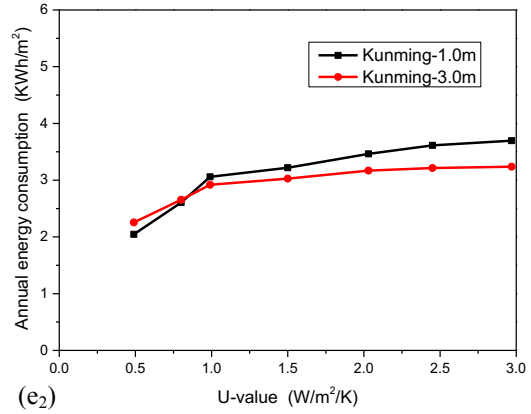
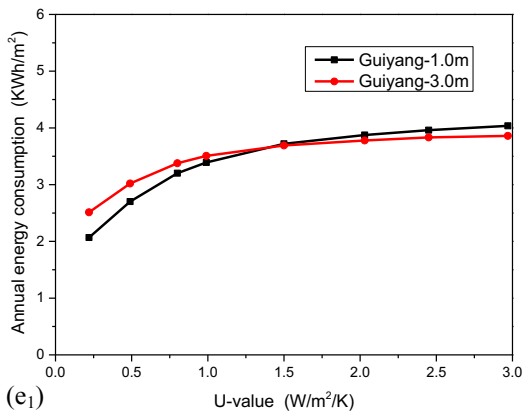
427

428

429

430

431



432 Fig.6 Relationships between annual energy demand and U-values of the roof for SCZ (a), CZ (b),

433 HSCWZ (c), HSWWZ (d), and TZ (e)

### 434 3.4 Impact of the thermal characteristics of the exterior wall

435 Fig.7 (a)-(e) depicts the relationships between the annual energy demand and the

436 U-values of the exterior wall in underground buildings for various climatic zones in

437 China. Overall, these relationships vary with changes in the climate.

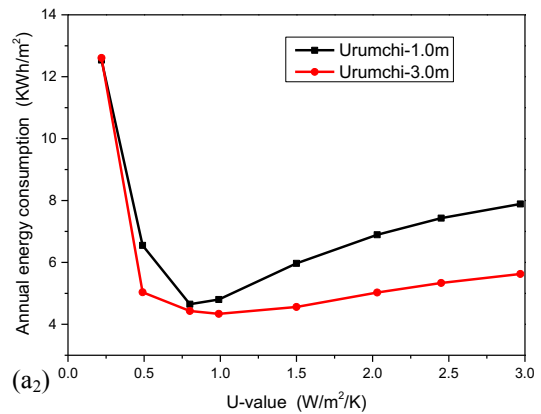
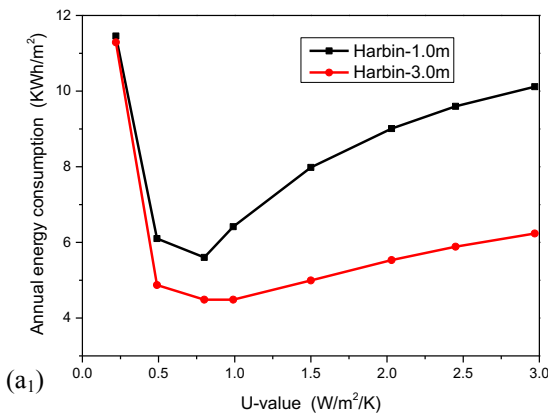
438

439

440

441

442



443

444

445

446



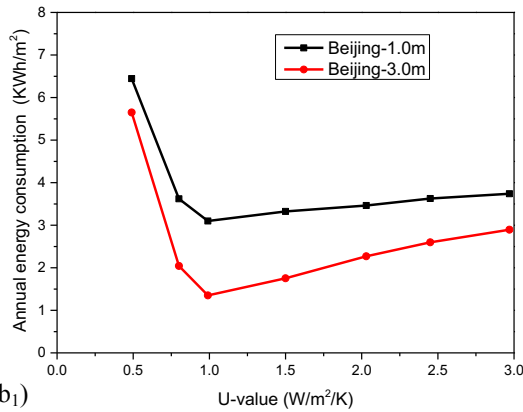
447

448

449

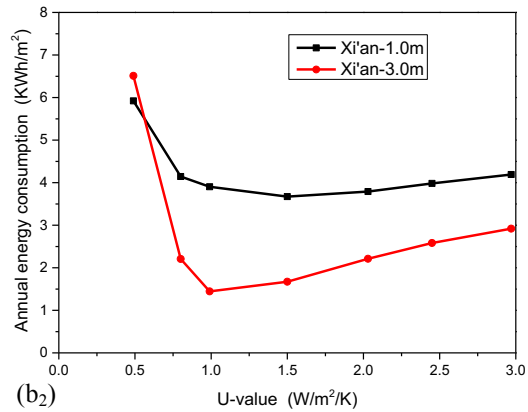
450

451



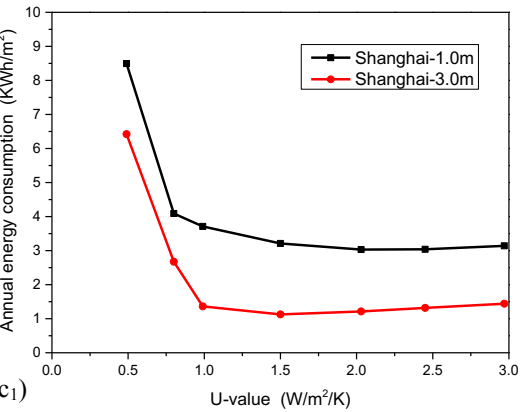
452

(b<sub>1</sub>)



(b<sub>2</sub>)

453

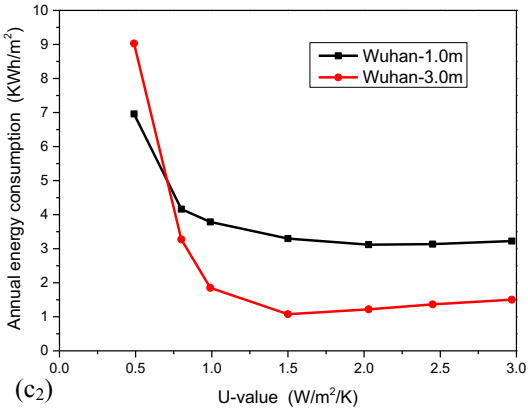


454

455

456

(c<sub>1</sub>)



(c<sub>2</sub>)

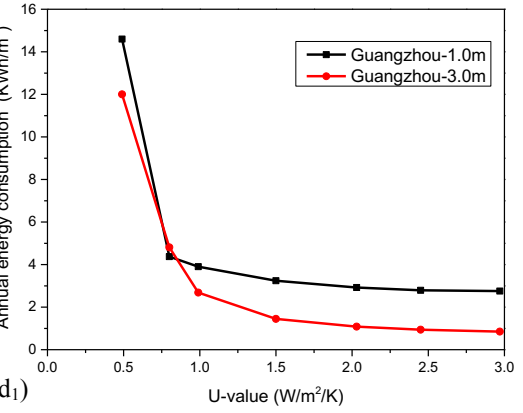
457

458

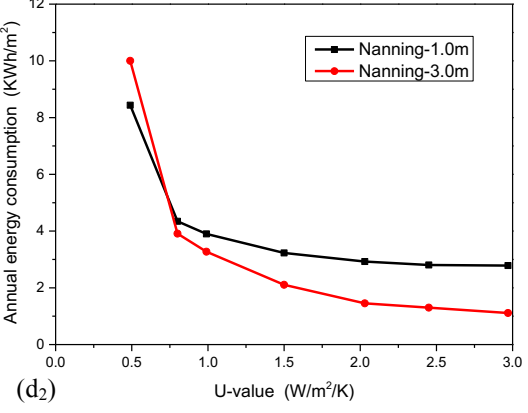
459

460

461



(d<sub>1</sub>)



(d<sub>2</sub>)

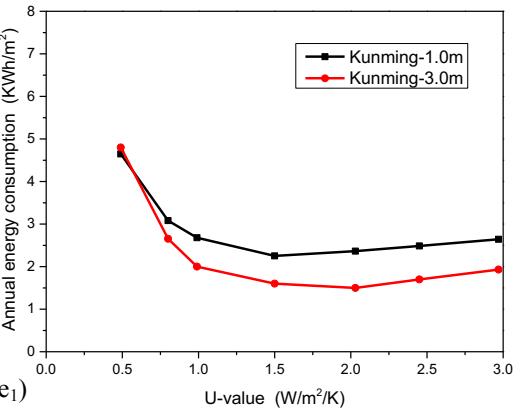
462

463

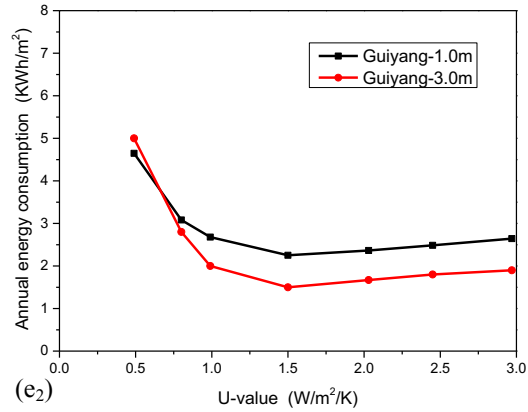
464

465

466



(e<sub>1</sub>)



(e<sub>2</sub>)

467

468 Fig.7 Relationships between annual energy demand and U-values of the exterior wall for SCZ (a), CZ

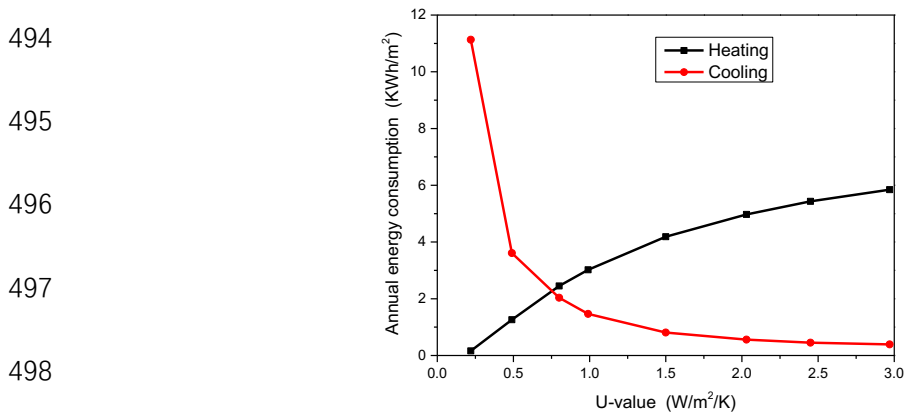
(b), HSCWZ (c), HSWWZ (d), and TZ (e)

469

470 A minimum is clearly observed in Fig.7 (a) and (b), thereby implying that there is  
471 an optimal U-value for the exterior wall for SCZ and CZ. With respect to SCZ, it is  
472 noted that increasing the U-value from  $0.22 \text{ W}/(\text{m}^2 \cdot \text{K})$  to  $0.8 \text{ W}/(\text{m}^2 \cdot \text{K})$  effectively  
473 reduces the annual energy consumption. However, this is followed by a continuous  
474 increase in the annual energy demand as a function of the U-value. Thus, the optimum  
475 U-value for the exterior wall for SCZ is approximately equal to  $0.8 \text{ W}/(\text{m}^2 \cdot \text{K})$ .  
476 Similarly, the optimum value of the exterior wall in an underground building for CZ is  
477  $1.0 \text{ W}/(\text{m}^2 \cdot \text{K})$ .

478 The reason pertaining to the achieved optimal level of the U-value of the exterior  
479 wall is attributed to the differential impacts of energy consumption owing to heating  
480 and cooling. Fig.8 shows the variations in heating and cooling energies as a function  
481 of the U-values of the exterior wall in Harbin. Specifically, the thermal resistance of  
482 the exterior wall effectively prevents heat from being transferred into the surrounding  
483 soil in winter. Nevertheless, if the U-value is excessively low, the heat generated in  
484 the room cannot be effectively transferred into the soil, and this leads to an increased  
485 cooling load. In the summer, a decrease in the U-value of the exterior wall can  
486 effectively transfer more heat into the surrounding soil, and this is helpful in yielding  
487 significant decreases in the indoor temperature and in the cooling load. Thus, a  
488 decrease in the U-value of the exterior wall is beneficial in the reduction of the  
489 heating energy in winter, while an increase in the U-value is helpful in reducing the  
490 cooling energy in the summer. It is necessary to evaluate a trade-off by considering

491 the optimal annual energy consumption (including the heating and cooling energies)  
492 when the thermal performance of the exterior wall in an underground building is  
493 designed for energy conservation.



499 Fig.8 Variations in the annual energy consumption for heating and cooling as a function of U-values of  
500 the exterior wall in Harbin

501 With respect to the HSCWZ, the optimized value was approximately 1.5 W/(m²·K),  
502 but when the U-value increased to 2.0 W/(m²·K), its impact on building energy  
503 consumption was minimized. Similarly, the optimized U-value for TZ was  
504 approximately in the range of 1.5–2.0 W/(m²·K), as shown in Fig.7 (e). It should be  
505 noted that higher U-values elicit lower annual energy demand for buildings in  
506 HSCWZ, even though the effectiveness of the U-value is not significant at higher  
507 values. This means that thermal insulation materials are not necessary for the exterior  
508 walls in underground buildings for HSCWZ, and that the U-value of the exterior walls  
509 should in general be larger than 2.0 W/(m²·K). These findings are completely  
510 different from those for buildings above the ground. The main reason for this  
511 difference is the soil temperature. Fig.9 presents the measured data of the soil  
512 temperature at a depth of 3.2 m in a typical underground building in five selected

513 cities corresponding to different climatic zones in China [29].

514

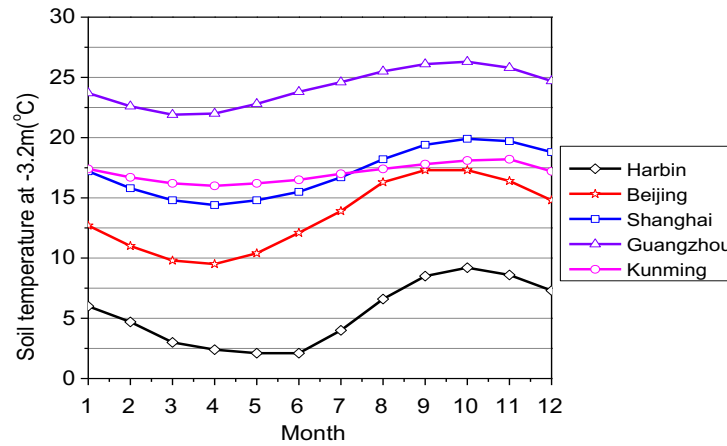
515

516

517

518

519



520

Fig. 9 Measured data of the soil temperature at a depth of 3.2 m below the ground

521

522

523

524

525

526

Based on Fig.9, it is observed that the average soil temperature corresponding to a depth of 3.2 m below the ground in Guangzhou (HSCWZ) reached 24 °C, and that the yearly dry-bulb temperature exceeded 20 °C. Thus, cooling of the interior space constitutes the main consequence in response to the climatic changes of HSWWZ. Increasing the U-value of the exterior wall is helpful in transferring the heat generated in the space into the surrounding soil.

527

528

529

530

531

532

533

534

Conversely, the fluctuation in the soil temperature in Harbin (SCZ) and Beijing (CZ) exceeded the corresponding fluctuations for the other three cities. For example, in Harbin, the average soil temperature (at a depth of 3.2 m below the ground) is the lowest among all the studied cities, and corresponded to approximately 5 °C. Thus, it is curial to reduce heat losses through the external walls. This is the reason why the basic requirements of good thermal insulation of the envelope need to be met for SCZ and CZ.

## 535 **4 Conclusions**

536 The focus of the present study is the thermal performance of the envelope for  
537 soil-buried office buildings, which may show distinct characteristics when compared  
538 to conventional buildings that are built above the ground. An advanced building  
539 energy-modelling tool (DeST) that accounted for the impact of the surrounding soil  
540 environment was used to simulate the building's energy performance in the case of a  
541 prototype underground building. The simulation results of the indoor air temperature  
542 for an underground meeting room were compared with the onsite long-term  
543 measurement data, and yielded a good agreement, thus demonstrating that dealing  
544 with the thermal process of an underground building using DeST is accurate and  
545 feasible. Most importantly, the hourly heating and cooling loads were calculated by  
546 DeST, the relationships between the annual energy consumption and the U-values of  
547 the envelopes were detected for various climates in China. The following conclusions  
548 can be drawn:

549 (1) The temperature waves between the indoor temperature of underground spaces  
550 and the outdoor climate differ in terms of values, amplitude, and phase displacement,  
551 owing to the high thermal capacity of the surrounding soil.

552 (2) Conversely, with respect to underground buildings, implementing a similar  
553 building energy efficiency strategy manifested by the decrease in the U-values of the  
554 envelopes (enhancing the thickness of thermal insulation), may result in an increased  
555 energy consumption when the thermal performance of the envelopes is designed for  
556 underground buildings.

557 (3) An improvement in the thermal performance of the roof plays an important role  
558 in reducing the energy demands for the underground office building. The energy  
559 efficiency requirements of roofs for the underground office buildings show  
560 consistency with the standard adopted for buildings that are above the ground

561 (4) The optimal U-values of an exterior wall for underground office buildings are  
562 completely different in the various climatic zones in China. For SCZ and CZ, the  
563 optimal U-values are  $0.8 \text{ W}/(\text{m}^2\cdot\text{K})$  and  $1.0 \text{ W}/(\text{m}^2\cdot\text{K})$ , respectively, while for  
564 HSCWZ and TZ, the recommended optimal values are in the range of  $1.5\text{--}2.0$   
565  $\text{W}/(\text{m}^2\cdot\text{K})$ . In terms of the building energy efficiency, thermal insulation is not  
566 required for HSWWZ.

567 These conclusions were drawn for soil-buried office buildings and the  
568 recommendations for optimal design U-values of building envelopes may not be  
569 suitable for other building functions. A further study should be carried out to  
570 investigate the impact of the thermal performance of building envelopes on annual  
571 energy consumption for various building functions, such as underground shopping  
572 malls, parking space, railways, hospitals, etc. In addition, the contact surface area of  
573 building with the earth plays a key role in heat transfer with underground buildings,  
574 and thus it is necessary to study the impact of contact surface area of building with the  
575 earth on the energy consumption and the optimal U-values of building envelopes, and  
576 further to correct these optimization results.

577

578 **5 Acknowledgment**

579 This study was financially supported by China Construction Engineering Design  
580 Group Corporation Limited (CSCEC-2014-Z-1-2).

581 **6 References**

582 [1] Nezhnikova E. The Use of Underground City Space for the Construction of Civil  
583 Residential Buildings [J]. Procedia Engineering, 2016, 165:1300-1304.

584 [2] Zhao JW, Peng FL, Wang TQ, et al. Advances in master planning of urban  
585 underground space (UUS) in China[J]. Tunnelling & Underground Space Technology  
586 Incorporating Trenchless Technology Research, 2016, 55:290-307.

587 [3] Yu RH, Ye QY. Review on the Development of Underground Shopping Mall in  
588 China[J]. Studies in Sociology of Science, 2012, 3(1).

589 [4] Shan M, Hwang BG, Wong KSN. A preliminary investigation of underground  
590 residential buildings: Advantages, disadvantages, and critical risks[J]. Tunnelling &  
591 Underground Space Technology, 2017, 70:19-29.

592 [5] He L, Song Y, Dai S, et al. Quantitative research on the capacity of urban  
593 underground space – The case of Shanghai, China[J]. Tunnelling & Underground  
594 Space Technology, 2012, 32(11):168-179.

595 [6] Staniec M, Nowak H. Analysis of the earth-sheltered buildings' heating and  
596 cooling energy demand depending on type of soil[J]. Archives of Civil & Mechanical  
597 Engineering, 2011, 11(1):221-235.

598 [7] Delmastro C, Lavagno E, Schranz L. Energy and underground[J]. Tunnelling &

599 Underground Space Technology Incorporating Trenchless Technology Research, 2016,  
600 55(2925):96-102.

601 [8] Alkaff S A, Sim S C, Efzan M N E. A review of underground building towards  
602 thermal energy efficiency and sustainable development[J]. Renewable & Sustainable  
603 Energy Reviews, 2016, 60:692-713.

604 [9] Al-Mumin AA. Suitability of sunken courtyards in the desert climate of Kuwait[J].  
605 Energy & Buildings, 2001, 33(2):103-111.

606 [10] Barker MB. Using the earth to save energy: Four underground buildings [J].  
607 Tunnelling & Underground Space Technology Incorporating Trenchless Technology  
608 Research, 1986, 1(1):59-65.

609 [11] Christian JE. Cooling season performance of an earth-sheltered office/dormitory  
610 building in Oak Ridge, Tennessee[J]. Klinicheskaia Meditsina, 1984,  
611 162(12):7049-7057.

612 [12] Wang F. Mathematical modeling and computer simulation of insulation systems  
613 in below grade applications. Conference Thermal Performance of the Exterior  
614 Envelopes of Buildings; 1979.

615 [13] Liu J, Jiang Y, Jin Y A. Dynamic Model of Heat Transfer through Underground  
616 Building Envelope[C]// International Conference on Intelligent System Design and  
617 Engineering Application. IEEE Computer Society, 2010:649-652.

618 [14] Choi S, Krarti M. Thermally optimal insulation distribution for underground  
619 structures[J]. Energy & Buildings, 2000, 32(3):251-265.

620 [15] Tinti F, Barbaresi A, Benni S, et al. Experimental analysis of shallow



621 underground temperature for the assessment of energy efficiency potential of  
622 underground wine cellars[J]. *Energy & Buildings*, 2014, 80:451-460.

623 [16] Peng C, Wang L, Zhang X. DeST-based dynamic simulation and energy  
624 efficiency retrofit analysis of commercial buildings in the hot summer/cold winter  
625 zone of China: A case in Nanjing[J]. *Energy & Buildings*, 2014, 78(4):123-131.

626 [17] Nielsen TR. Simple tool to evaluate energy demand and indoor environment in  
627 the early stages of building design[J]. *Solar Energy*, 2005, 78(1):73-83.

628 [18] Lin YH, Tsai KT, Lin MD, et al. Design optimization of office building envelope  
629 configurations for energy conservation[J]. *Applied Energy*, 2016, 171:336-346.

630 [19] ASHRAE, ANSI/ASHRAE Standard 90.1—2010: Energy Standard for Building  
631 except Low-rise Residential Buildings, ASHRAE, Atlanta, GA, 2010.

632 [20] Design Standard for Energy Efficiency of Public Buildings. China Architecture  
633 and Building Press; 2015.

634 [21] Ma X, Cheng B, Peng G, et al. A numerical simulation of transient heat flow in  
635 double layer wall sticking lining envelope of shallow earth sheltered buildings[C]//  
636 International Joint Conference on Computational Sciences and Optimization. IEEE,  
637 2009:195-198.

638 [22] Yuan Y, Cheng B, Mao J, et al. Effect of the thermal conductivity of building  
639 materials on the steady-state thermal behavior of underground building envelopes[J].  
640 *Building & Environment*, 2006, 41(3):330-335.

641 [23] Staniec M, Nowak H. Analysis of the energy performance of –earth-sheltered  
642 houses with southern elevation exposed [J].

- 643 [24] Cui Y, Yan D, Hong T, et al. Comparison of typical year and multiyear building  
644 simulations using a 55-year actual weather data set from China[J]. Applied Energy,  
645 2017, 195.
- 646 [25] Yan D, Xia J, Tang W, et al. DeST — An integrated building simulation toolkit  
647 Part I: Fundamentals[J]. Building Simulation, 2008, 1(2):95-110.
- 648 [26] Xie X, Jiang Y, Xia J. A new approach to compute heat transfer of  
649 ground-coupled envelope in building thermal simulation software[J]. Energy &  
650 Buildings, 2008, 40(4):476-485.
- 651 [27] Zhang H, Liu J, Li C, et al. Long-term investigation of moisture environment in  
652 underground civil air defense work[J]. Indoor & Built Environment, 2016.
- 653 [28] Xie XN, Song FT, Zhang XL, et al. Building environment design simulation  
654 software DeST (11): treatment of dynamic heat transfer through underground zone[J].  
655 Heating Ventilating & Air Conditioning. 2005, 35(6):55-63.
- 656 [29] Organization of Chinese Architecture Standards Design Institute. Design manual  
657 for air defense basement: HVAC[M].2006.